

THE APPLICATION OF THE MODIFIED FORM OF BÄTH'S LAW TO THE NORTH ANATOLIAN FAULT ZONE (NAFZ), AEGEAN GRABEN SYSTEM AND CYPRUS ARC ZONE

Sibel Ebru YALCIN¹, Levent KURNAZ²

Abstract

Earthquakes and aftershock sequences follow several empirical scaling laws: (1) Gutenberg-Richter frequency-magnitude scaling, (2) Båth's law for the magnitude of the largest aftershock, (3) The modified Omori's law for the temporal decay of aftershocks. In this paper, "The Modified Form of Båth's Law" and its application to our KOERI data have been studied. Båth's law states that the differences in magnitudes between mainshocks and their largest aftershocks are approximately constant, independent of the magnitudes of mainshocks. In the modified form of Båth's law for a given mainshock we get the inferred "largest" aftershock of this mainshock by using an extrapolation of the Gutenberg-Richter frequency-magnitude statistics of the aftershock sequence. To test the applicability of the modified form of Båth's Law we consider 14 large earthquakes that occurred in and near boundary neighbors of Turkey between 1900 and 2004 with magnitudes equal to or greater than $m_{ms} \geq 6.1$. Because Turkey has different fault zones that have different properties, a classification was needed for these earthquakes. Additionally, in this study the partitioning of energy during a mainshock-aftershock sequence was also calculated in two different ways. It is shown that most of the energy is released in the mainshock. The constancy of the differences in magnitudes between mainshocks and their largest aftershocks is an indication of scale-invariant behavior of aftershock sequences.

Introduction

An earthquake is a sudden and sometimes catastrophic movement of a part of the Earth's surface [1]. It is caused by the release of stress accumulated along geologic faults or by volcanic activity, hence the earthquakes are the Earth's natural means of releasing stress. When the Earth's plates move against each other, stress is put on the lithosphere. When this stress is strong enough, the lithosphere breaks or shifts. As the plates move they put forces on themselves and each other. When the force is large enough, the crust is forced to break. When the break occurs, the stress is released as energy which moves through the Earth in the form of waves, which we feel and call an earthquake.

There are several scaling laws that describe the statistical properties of aftershock sequences [2, 3, 4]. Gutenberg-Richter frequency-magnitude scaling law is widely known by seismologists and scientists. In order to study the noise of earthquakes, we must first find a way to measure the sizes of earthquakes. Charles Richter developed the main scale that is used today. On the Richter scale, the magnitude (M) of an earthquake is proportional to the log of the maximum amplitude of the earth's motion. What this mean is that if the earth moves one millimeter in a magnitude 2 earthquake, it will move 10 millimeters in a magnitude 3 earthquake, 100 millimeters in a magnitude 4 earthquake and 10 meters in a

¹ Bogazici University, Physics Department, Bebek, İstanbul, TURKEY, syalcin@physics.umass.edu

² Bogazici University, Physics Department, Bebek, İstanbul, TURKEY, kurnaz@boun.edu.tr

magnitude 6 earthquake. Therefore, if we hear about a magnitude 8 earthquake and a magnitude 4 earthquake, we know that the ground is moving 10,000 times more in the magnitude 8 earthquake than in the magnitude 4 earthquake. The difference in energies is even greater. For each factor of 10 in amplitude, the energy grows by a factor of 32, so a magnitude 8 earthquake releases 1,000,000 times more energy than a magnitude 4 earthquake. When seismologists started measuring the magnitudes of earthquakes, they found that there were a lot more small earthquakes than large ones. Seismologists have found that the earthquakes of magnitude M is proportional to 10^{-bM} . They call this law "The Gutenberg-Richter Law".

In seismological studies, the Omori law, proposed by Omori in 1894, is one of the few basic empirical laws[6]. This law describes the decay of aftershock activity with time. Omori law and its modified forms have been used widely as a fundamental tool for studying aftershocks[7]. An extension of the modified Omori's law is the epidemic type of aftershock sequences (ETAS) model. It is a stochastic version of the modified Omori law. In the ETAS model, the rate of aftershock occurrence is an effect of combined rates of all secondary aftershock subsequences produced by each aftershock [9, 10].

The third scaling law relating the aftershocks is Båth's law. The empirical Båth's law states that the differences in magnitude between a mainshock and its largest aftershock is constant, regardless of the mainshock magnitude. That is

$$\Delta m = m_{ms} - m_{as}^{max} \quad (1)$$

with m_{ms} the magnitude of the mainshock, m_{as}^{max} the magnitude of the largest detected aftershock, and Δm approximately a constant and taken to be $\Delta m \approx 1.2$. [3, 4, 7, 8]

In this article we study on the modified form of Båth's law [3, 4]. To study the aftershock sequence in the North Anatolian Fault Zone (NAFZ) we get the largest aftershock from an extrapolation of the G-R frequency-magnitude scaling of all measured aftershocks. We test the applicability of Båth's law for 14 large earthquakes on the North Anatolian Fault Zone (NAFZ) and near the NAFZ. The empirical form of Båth's law states that the difference magnitude between a mainshock and its largest aftershock is constant, independent of the magnitudes of mainshocks. We also analyze the partitioning of energy during a mainshock-aftershock sequence and its relation to the modified Båth's law.

Båth's Law and Its Modified Form

Båth's law states that the differences in magnitudes between mainshocks and their largest aftershocks are approximately constant, independent of the magnitudes of mainshocks. In modified form of Båth's law for a given mainshock we get the inferred largest aftershock of this mainshock by using an extrapolation of the Gutenberg-Richter frequency-magnitude statistics of the aftershock sequence. The size distribution of earthquakes has been found to show a power law behavior: *Gutenberg and Richter*, introduced the common description of the frequency of earthquakes: [5]

$$\text{Log}_{10}N(\geq m) = a - bm \quad (2)$$

where $N(\geq m)$ is the cumulative number of earthquakes with magnitudes greater than m occurring in a specified area and time window, On this equation a and b are constants. This relation is valid for earthquakes with magnitudes above some lower cutoff m_c . Earlier studies [3, 4, 11] gave an estimate for this b value between 0.8 and 1.2. In our data, b is found to vary between 0.6 and 1.3, consistent with previous work. The constant a shows the regional level of seismicity and gives the logarithm of the number of earthquakes with magnitudes greater than zero. In our analysis a value is in the range $3.5 < a < 6.9$. Aftershocks related with a mainshock also satisfy G-R scaling (2) to a good approximation [3, 4]. In this case $N(\geq m)$ is the cumulative number of aftershocks of a given mainshock with magnitudes greater than m . We offer to extrapolate G-R scaling (2) for aftershocks. Our aim is to obtain an upper cutoff magnitude in a given aftershock sequence. We find the magnitude of this inferred "largest" aftershock m^* by formally taking $N(\geq m^*) = 1$ for a given aftershock sequence. Then, we substitute this value into equation (2), and we get

$$a = bm^* \quad (3)$$

This extrapolated m^* value will have a mean value and a standard deviation from the mean value. We apply the Bâth's law to the inferred values of m^* and then, we can write

$$\Delta m^* = m_{ms} - m^* \quad (4)$$

where m_{ms} is the magnitude of the mainshock and Δm^* is approximately a constant. Substitution of equations (3) and (4) into equation (2) gives

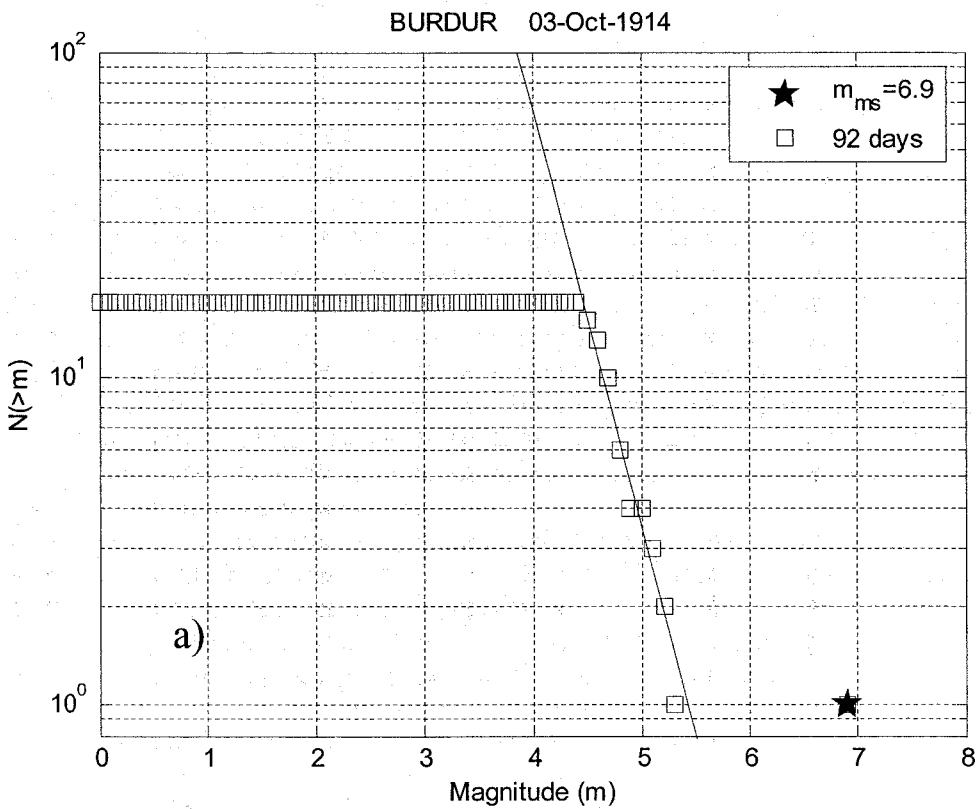
$$\text{Log}_{10} N[(\geq m)] = b(m_{ms} - \Delta m^* - m) \quad (5)$$

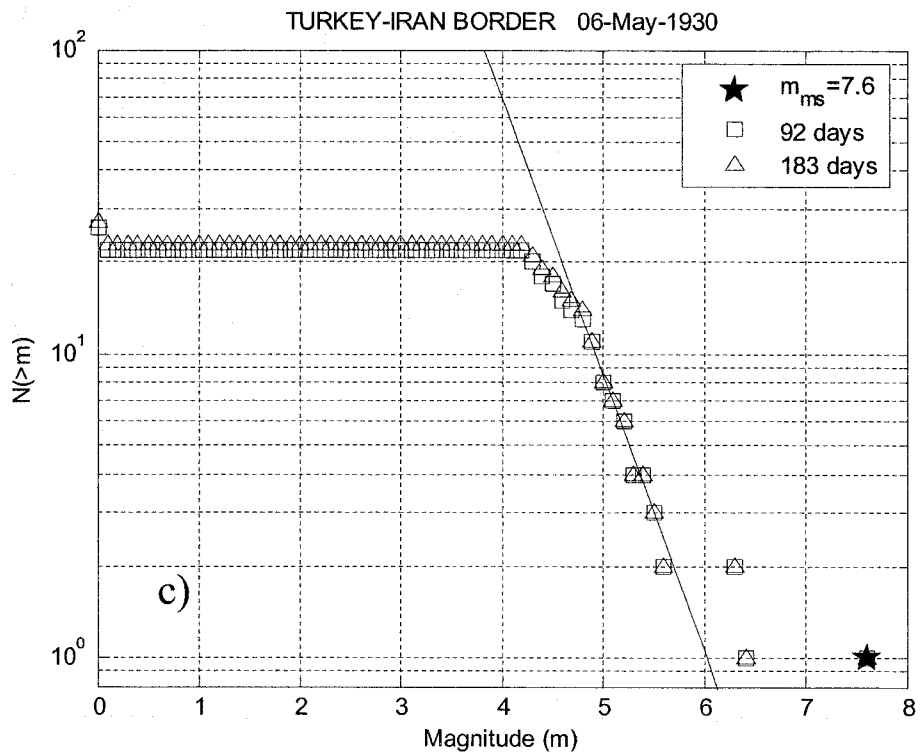
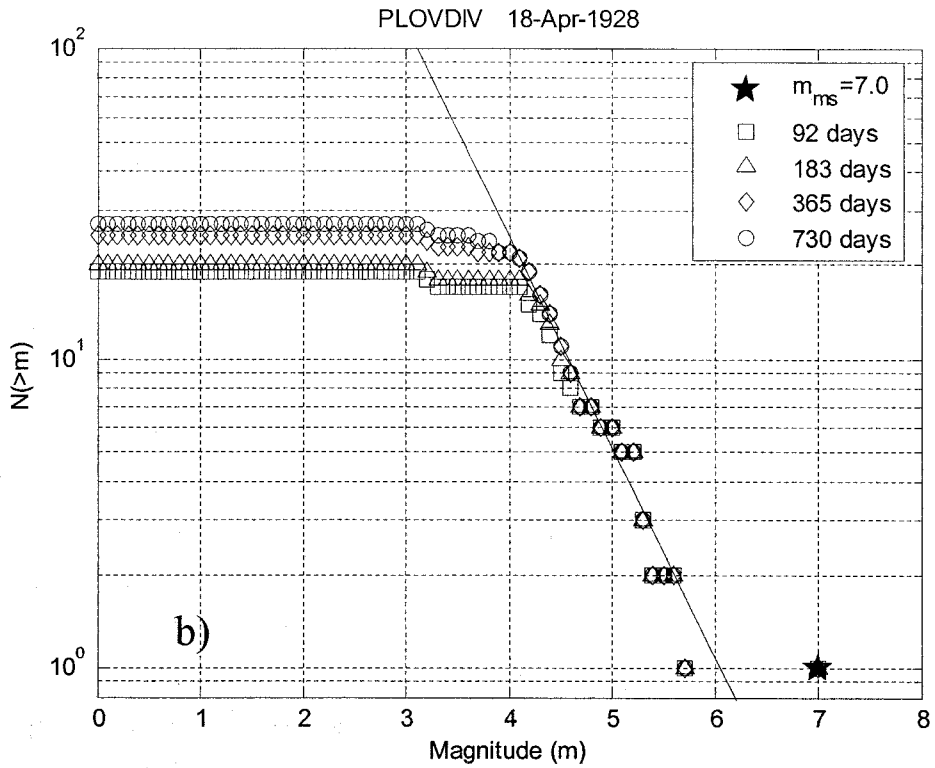
with b , m_{ms} , Δm^* specified, the frequency-magnitude distribution of aftershocks can be determined using equation (5). In extrapolating the G-R scaling (2) the slope of this scaling or b -value plays an important role in estimating the largest inferred magnitude m^* .

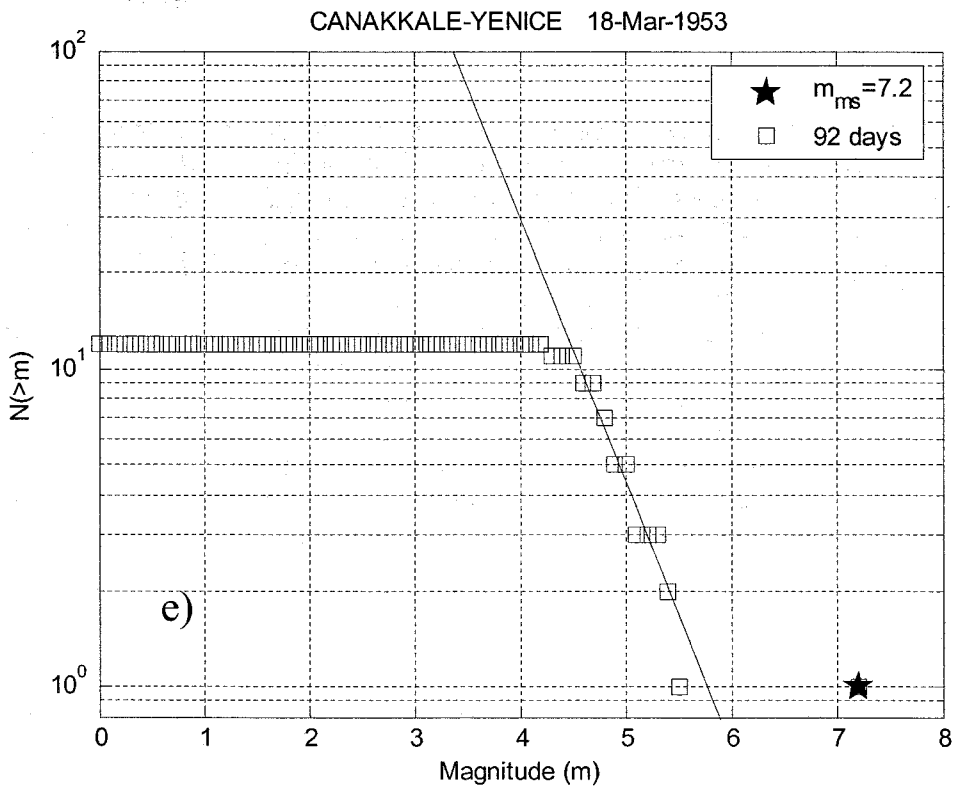
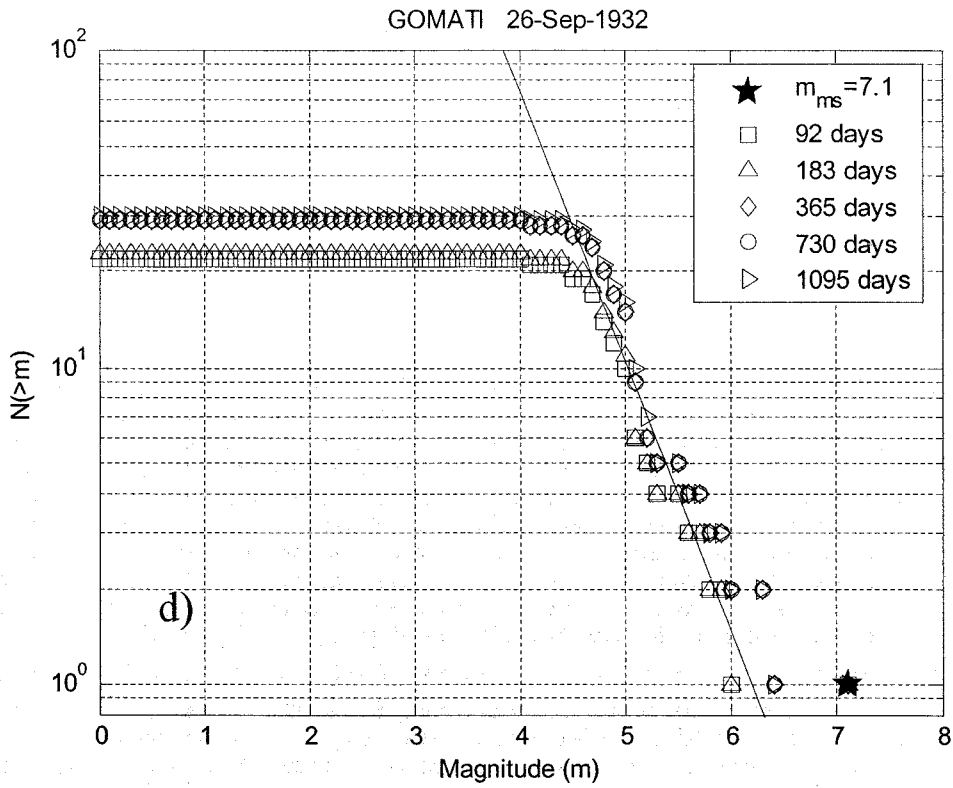
The Application of The Modified Form of Bâth's Law to Turkey

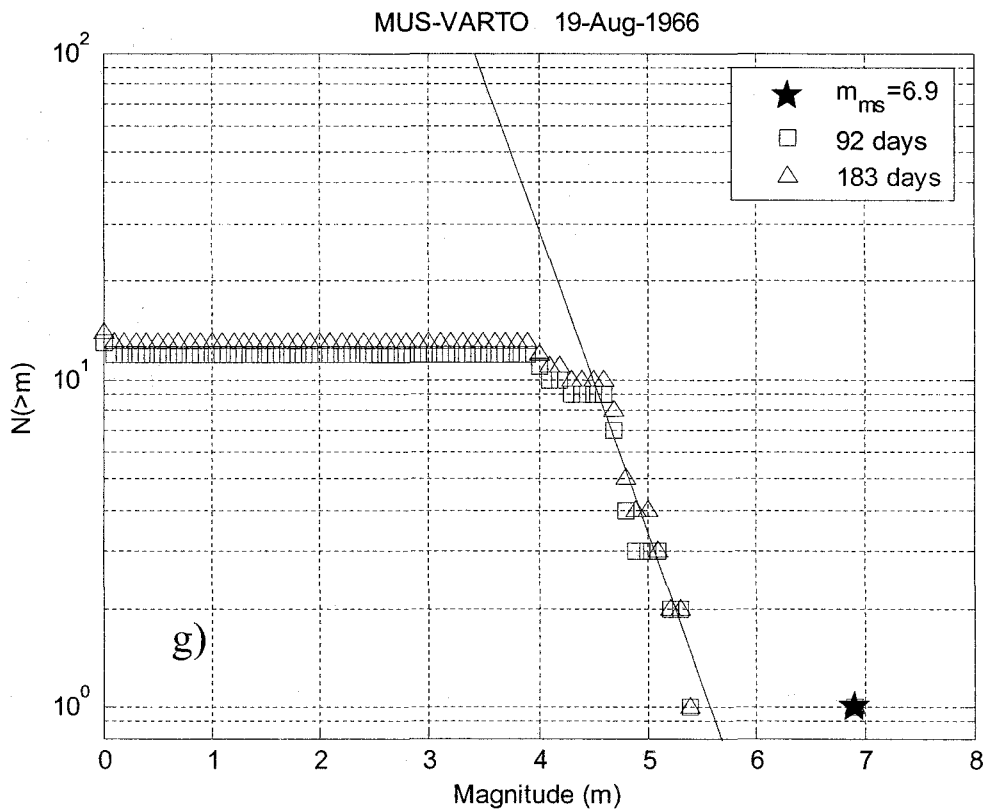
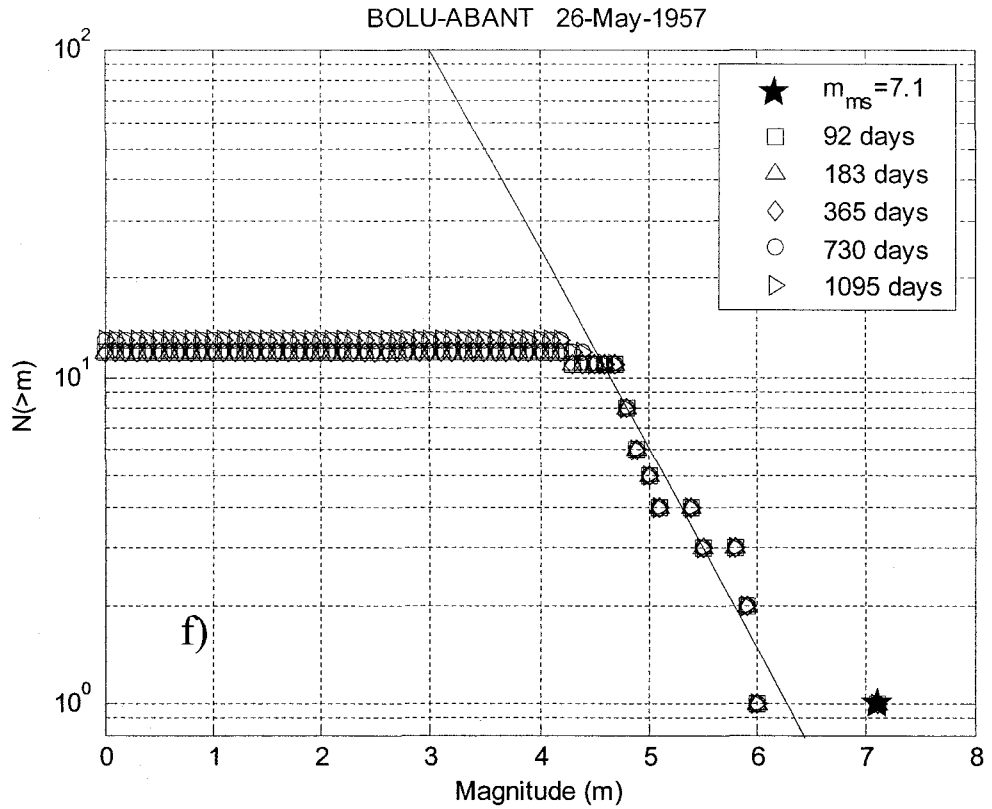
We applied modified form of Bâth's law by considering 14 large earthquakes in and near boundary neighbors of Turkey. These earthquakes occurred between 1900 and 2004. The data are provided by Bogazici University Kandilli Observatory and Earthquake Research Institute (<http://www.koeri.boun.edu.tr>) [12]. The 14 earthquakes considered had magnitudes $m_{ms} \geq 6.1$. The important point is that they were sufficiently separated in space and time so that no aftershock sequences overlapped with other mainshocks. Earthquakes form a hierarchical structure in space and time. Therefore, in some cases it is possible to discriminate foreshocks, mainshocks, and aftershocks. But, generally this classification is not well defined and can be ambiguous. One of our main problems in the study of aftershocks is to identify what is and what is not an aftershock [13]. To specify aftershocks we defined

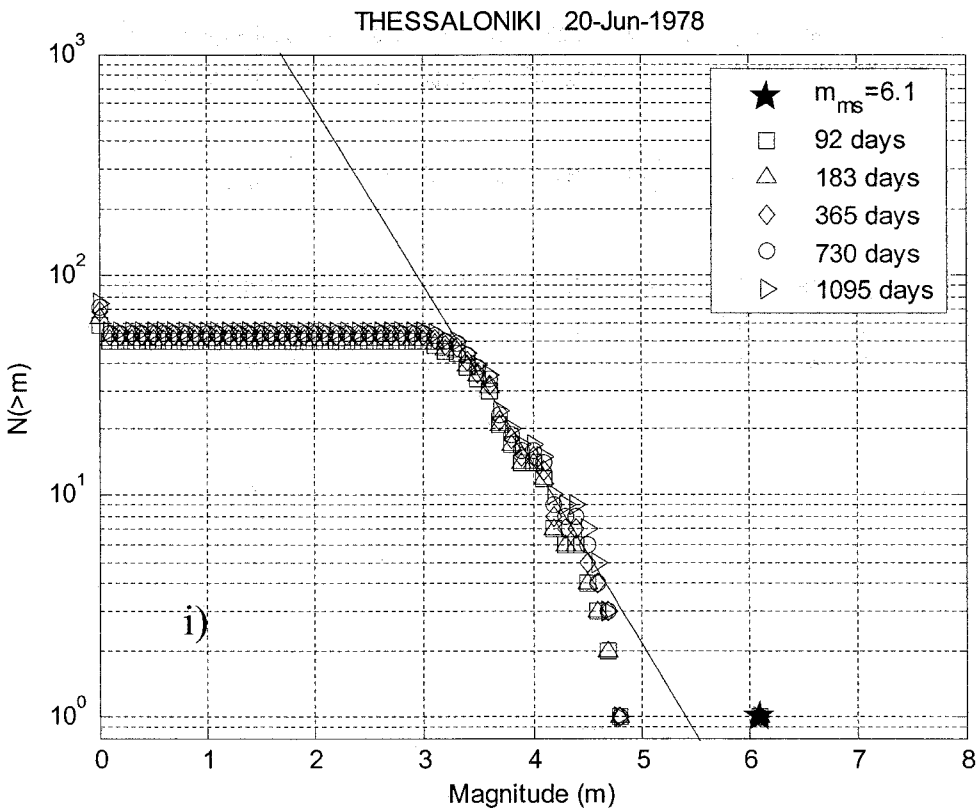
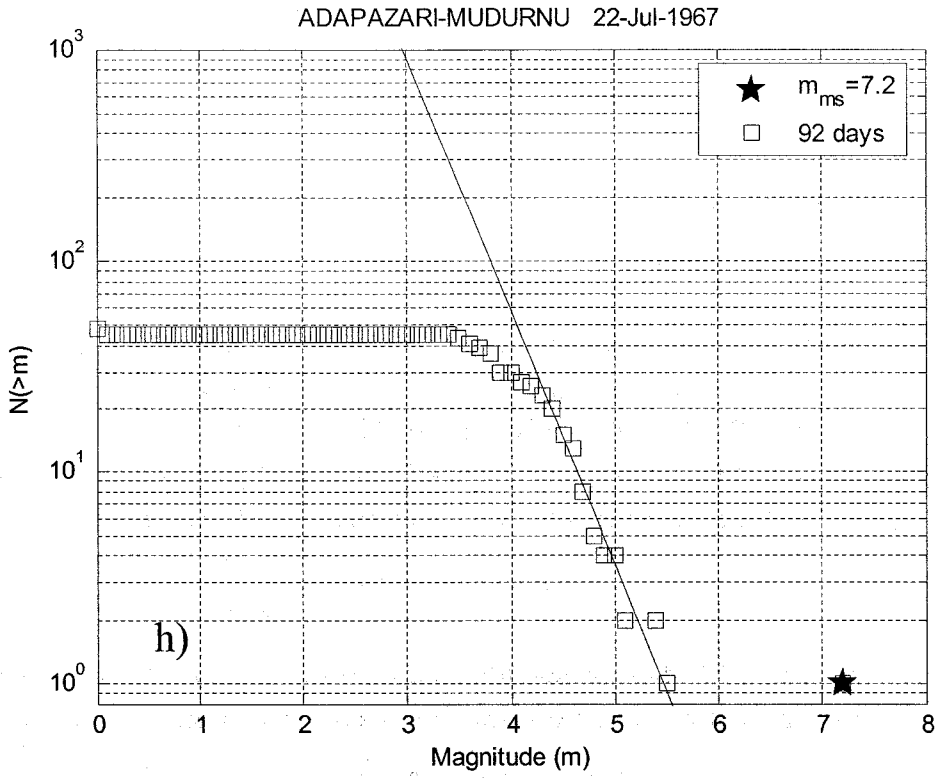
space and time windows for each sequence. In each case we consider a square area centered on the mainshock epicenter. The linear size of the box is taken to be of the order of the linear extent of the aftershock zone L , which scales with the magnitude of the mainshock m_{ms} as $L = 0.02 * 10^{0.5m_{ms}} \text{ km}$ [14]. Time intervals of 92, 183, 365, 730, and 1095 days are taken except Burdur, Plovdiv, Turkey-Iran Border, Canakkale-Yenice, Mus-Varto, Adapazari-Mudurnu earthquakes. It should also be noted that for all 14 earthquakes we took m_L , Richter magnitudes. The frequency-magnitude statistics for each case are shown in Figure 2.

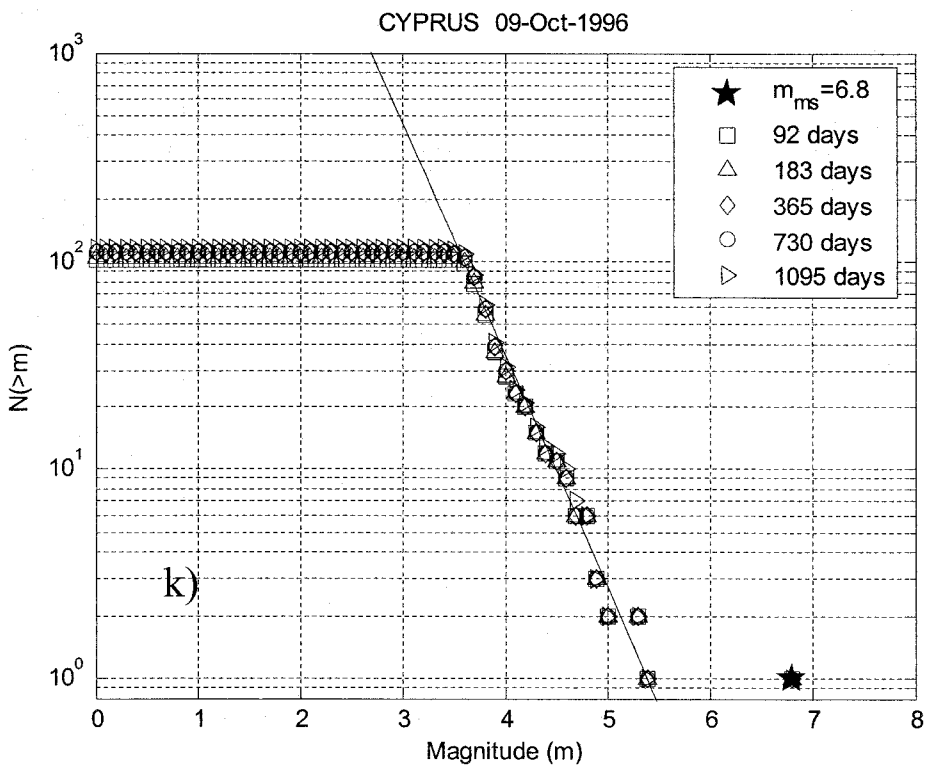
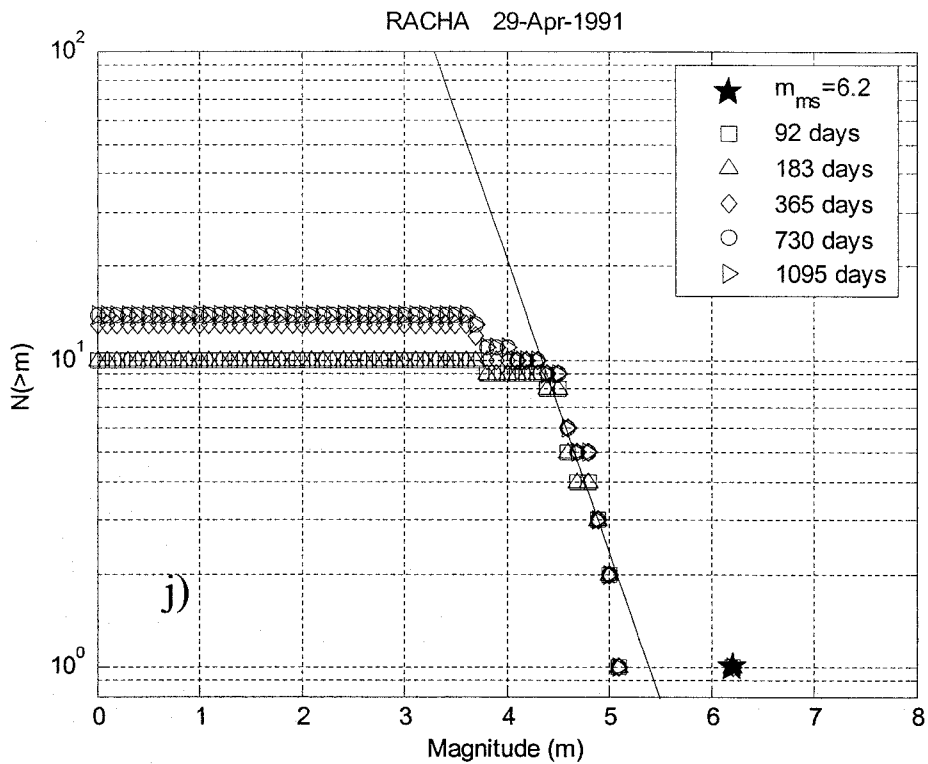


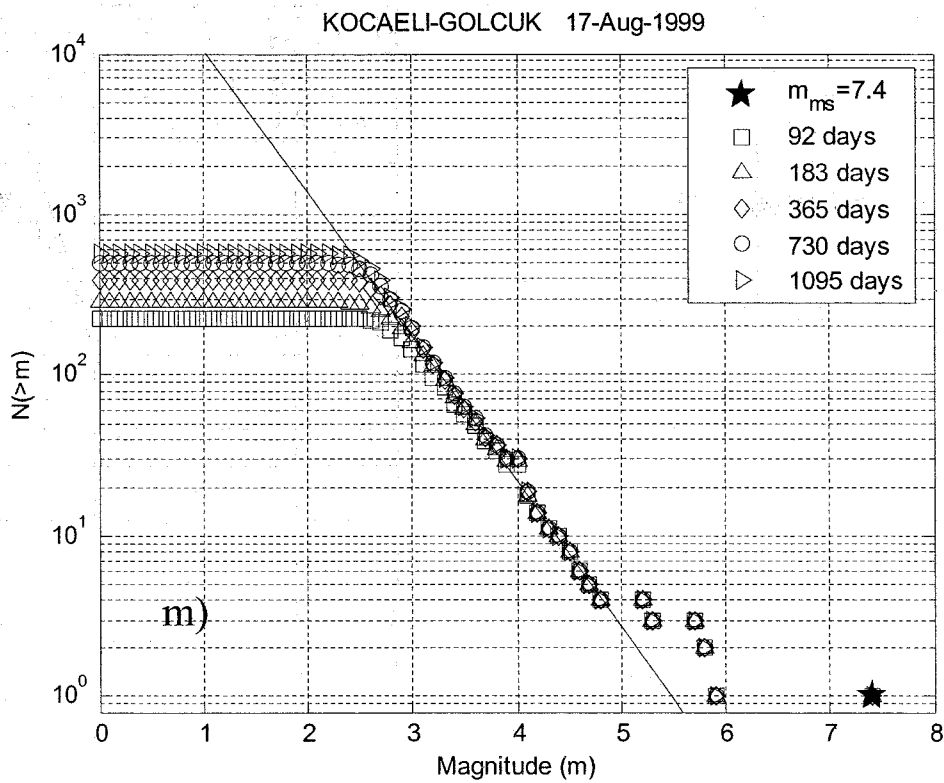
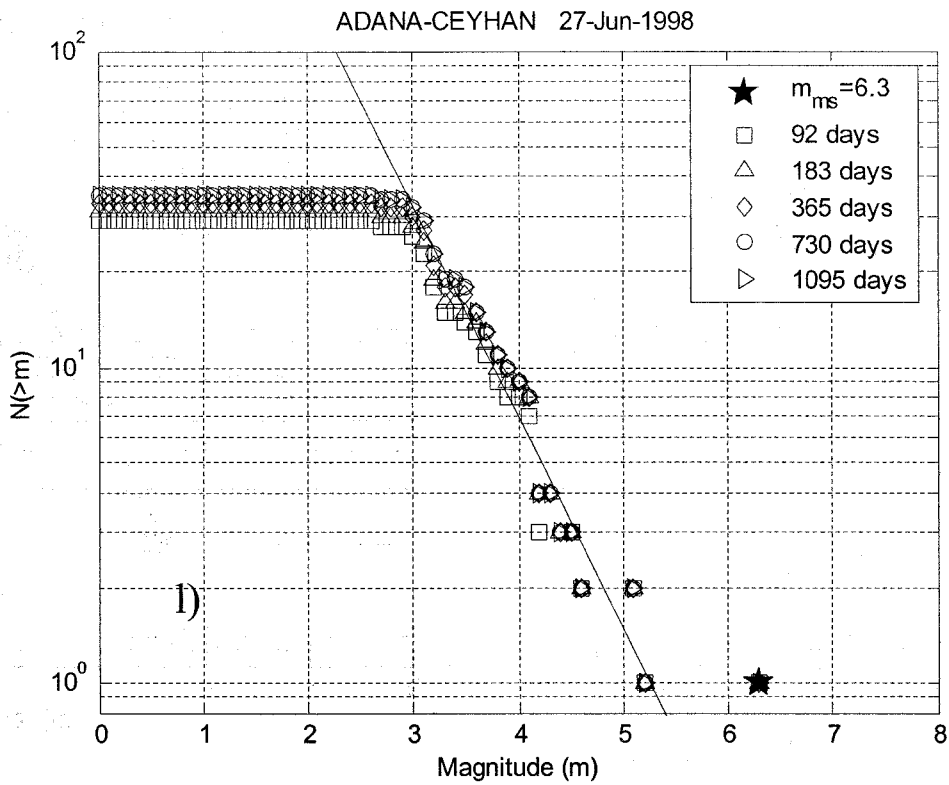












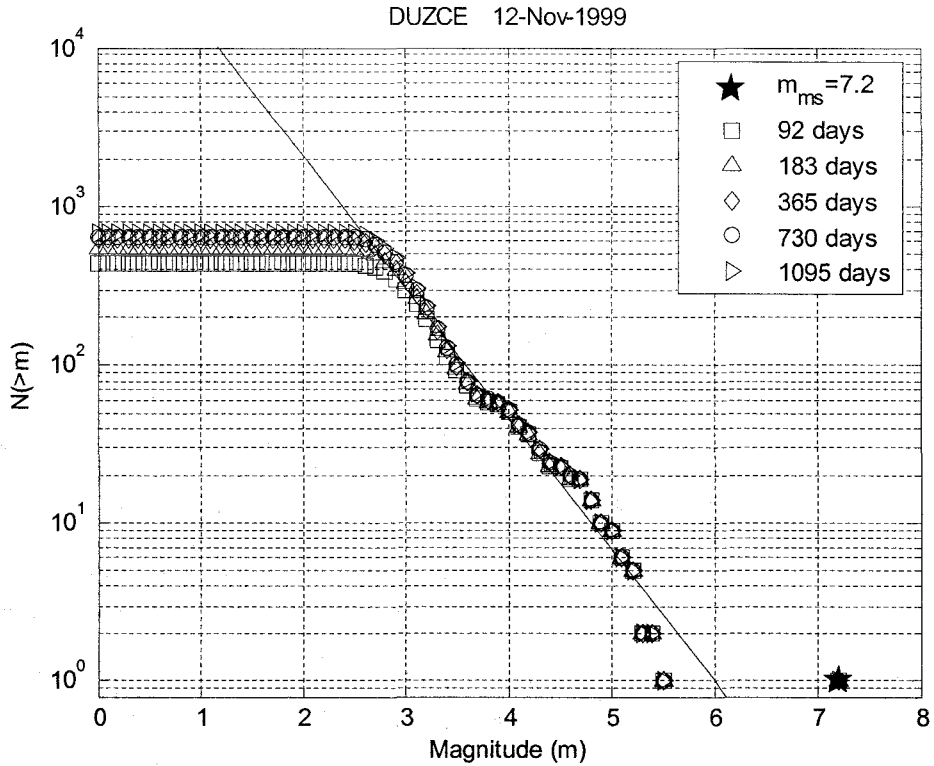


Figure 2. Frequency-magnitude distribution of Burdur (a), Plovdiv (b), Turkey-Iran Border (c), Gomati (d), Canakkale-Yenice (e), Bolu-Abant, (f) Mus-Varto (g), Adapazari-Mudurnu (h), Thessaloniki (i), Racha (j), Cyprus (k), Adana-Ceyhan (l), Kocaeli-Golcuk (m), and Duzce (n) earthquakes with magnitudes greater than m . The straight lines are the best-fits of equation (5) to data. The time period of 92 days following the mainshock was used for Burdur (a), Canakkale-Yenice (e), Adapazari-Mudurnu (h) earthquakes. The time periods of 92 and 183 days following the mainshock were used for Turkey-Iran Border (c) and Mus-Varto (g) earthquakes. The time periods of 92, 183, 365, 730 days following the mainshock were used for Plovdiv earthquake. The time periods of 92, 183, 365, 730, and 1095 days following the mainshock were used for the other earthquakes.

It should be noted that these 14 earthquakes take place on different fault zones in Turkey. So, we needed to make a classification for them with respect to their place. The $a, b, \Delta m, \Delta m^*, m_{ms}, m_{as}^{max}, m^*, \Delta m^*$ values for these earthquakes are given in Table 1 and Table 2.

Table 1
Summary of the Data and Results

Earthquake	Date (mm/dd/yy)	b	a
Burdur	10/03/14	1.28±0.02	6.94±0.09
Plovdiv	04/18/28	0.68±0.03	4.11±0.17
Turkey-Iran Border	05/06/30	0.91±0.03	5.48±0.14
Gomati	09/26/32	0.85±0.02	5.27±0.13
Canakkale-Yenice	03/18/53	0.83±0.02	4.79±0.12
Bolu-Abant	05/26/57	0.61±0.01	3.83±0.05
Mus-Varto	08/19/66	0.93±0.05	5.18±0.25
Adapazarı-Mudurnu	07/22/67	1.20±0.04	6.56±0.19
Thessaloniki	06/20/78	0.81±0.05	4.38±0.14
Racha	04/29/91	0.95±0.03	5.12±0.16
Cyprus	10/09/96	1.11±0.01	5.99±0.07
Adana-Ceyhan	06/27/98	0.67±0.03	3.52±0.13
Kocaeli-Golcuk	08/17/99	0.90±0.03	4.94±0.15
Duzce	11/12/99	0.83±0.02	4.98±0.09

Table 2
Summary of the Data and Results

Earthquake	Date (mm/dd/yy)	m_{ms}	m_{as}^{max}	Δm	m^*	Δm^*
Burdur	10/03/14	6.9	5.2	1.7	5.44±0.11	1.46±0.11
Plovdiv	04/18/28	7.0	5.6	1.4	6.03±0.38	0.97±0.38
Turkey-Iran Border	05/06/30	7.6	6.3	1.3	6.03±0.24	1.57±0.24
Gomati	09/26/32	7.1	5.9	1.2	6.18±0.19	0.92±0.19
Canakkale-Yenice	03/18/53	7.2	5.4	1.8	5.79±0.22	1.41±0.22
Bolu-Abant	05/26/57	7.1	5.9	1.2	6.25±0.12	0.85±0.12
Mus-Varto	08/19/66	6.9	5.3	1.6	5.58±0.39	1.32±0.39
Adapazarı-Mudurnu	07/22/67	7.2	5.4	1.8	5.45±0.23	1.75±0.23
Thessaloniki	06/20/78	6.1	4.7	1.4	5.40±0.35	0.70±0.35
Racha	04/29/91	6.2	5.0	1.2	5.40±0.23	0.80±0.23
Cyprus	10/09/96	6.8	5.3	1.5	5.38±0.09	1.42±0.09
Adana-Ceyhan	06/27/98	6.3	5.1	1.2	5.25±0.28	1.05±0.28
Kocaeli-Golcuk	08/17/99	7.4	5.8	1.6	5.50±0.27	1.90±0.27
Duzce	11/12/99	7.2	5.4	1.8	6.03±0.18	1.17±0.18

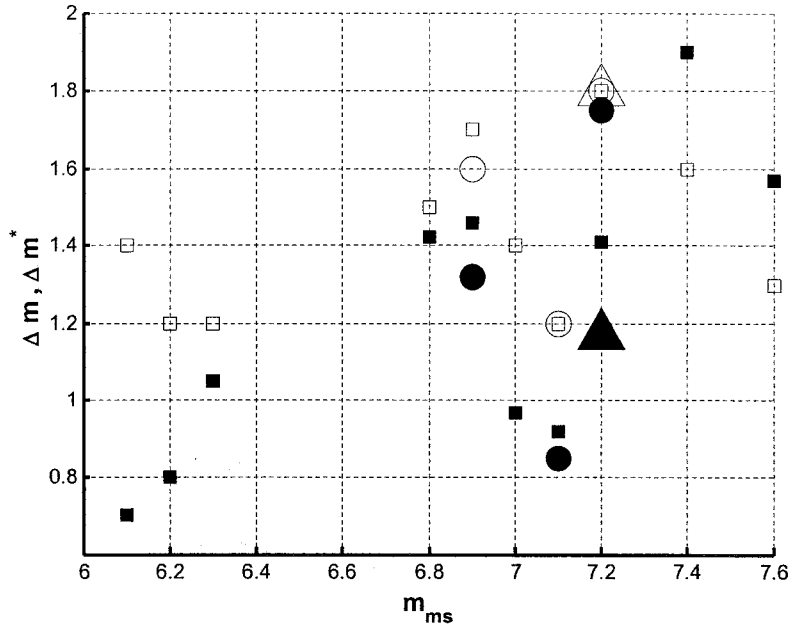


Figure 3. Dispersion of the magnitude differences Δm and Δm^* on the mainshock magnitude m_{ms} for the 14 earthquakes considered. In 14 earthquakes three of them have a magnitude of $m_{ms}=7.2$. Two of them have magnitude of $m_{ms}=6.9$ and two of them have magnitude of $m_{ms}=7.1$. Because of preventing the coincidences in this figure square, circle, and triangle were used. □, ○, △ correspond to Δm value. ■, ●, ▲ correspond to Δm^* value

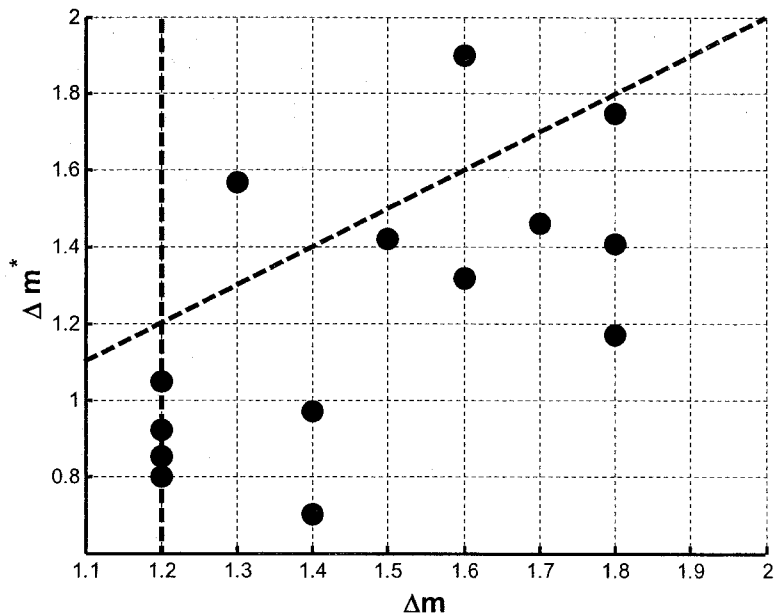


Figure 4. The relation between Δm and Δm^* . It shows the dependence of the inferred magnitude difference between the mainshock and the largest aftershock Δm^* on the actual magnitude differences Δm between the mainshock and the largest observed aftershock. In Figure 4, line 1 shows the harmony of our data with the Båth's Law. Line 2 corresponds to $y=x$ line and shows the harmony of our data with the Modified Form of Båth's Law.

Classifying Earthquakes According To Fault Zones

Because Turkey has many fault zones that have different properties, we did not evaluate all 14 earthquakes in the same category. We tried to make a classification among them with respect to their mainshock epicenter. Turkey is located on the relatively small Anatolian plate, which is squeezed between three other major tectonic plates, the north-moving African and Arabian plates located to the south, and the south-moving Eurasian plate located to the north. The combination of these plate movements is forcing the Anatolian plate to move west into the Aegean Sea. This movement produces fault structures at the boundary between the plates, most significantly the North Anatolian Fault Zone (NAFZ) and the East Anatolian Fault Zone (EAFZ).

According to our classification, six earthquakes take place on the North Anatolian Fault Zone (NAFZ). They are Canakkale-Yenice, Bolu-Abant, Mus-Varto, Adapazari-Mudurnu, Kocaeli-Golcuk, and Duzce earthquakes. One earthquake is on the East Anatolian Fault Zone (EAFZ). It is Turkey-Iran Border earthquake. One earthquake is in Georgia. This is the Racha earthquake. Four earthquakes take place on Aegean Graben System. These are Burdur, Plovdiv, Gomati, Thessaloniki earthquakes. And finally two earthquakes are on Cyprus Arc Zone. They are Cyprus and Adana-Ceyhan earthquakes.

For the earthquakes that are on the North Anatolia Fault Zone (NAFZ), the mean of the differences between mainshock and largest detected aftershock magnitudes is $\overline{\Delta m} = 1.63$ with a standard deviation $\sigma_{\overline{\Delta m}} = 0.23$. The mean of the inferred values of Δm^* obtained from the best fit of equation (5) is $\overline{\Delta m^*} = 1.20$ with a standard deviation $\sigma_{\overline{\Delta m^*}} = 0.08$. In addition for these earthquakes the mean of b values is $\overline{b} = 0.72$ with a standard deviation $\sigma_{\overline{b}} = 0.01$.

For the earthquakes that are on Aegean Graben System, the mean of the differences between mainshock and largest detected aftershock magnitudes is $\overline{\Delta m} = 1.43$ with a standard deviation $\sigma_{\overline{\Delta m}} = 0.21$. The mean of the inferred values of Δm^* obtained from the best fit of equation (5) is $\overline{\Delta m^*} = 1.30$ with a standard deviation $\sigma_{\overline{\Delta m^*}} = 0.09$. In addition for these earthquakes the mean of b values is $\overline{b} = 0.98$ with a standard deviation $\sigma_{\overline{b}} = 0.01$.

For the earthquakes that are on Cyprus Arc Zone, the mean of the differences between mainshock and largest detected aftershock magnitudes is $\overline{\Delta m} = 1.35$ with a standard deviation $\sigma_{\overline{\Delta m}} = 0.21$. The mean of the inferred values of Δm^* obtained from the best fit of equation (5) is $\overline{\Delta m^*} = 1.39$ with a standard deviation $\sigma_{\overline{\Delta m^*}} = 0.09$. In addition for these earthquakes the mean of b values is $\overline{b} = 1.10$ with a standard deviation $\sigma_{\overline{b}} = 0.01$.

Partitioning of Energy Among Mainshock and Aftershock Sequences

Seismologists have more recently developed a standard magnitude scale that is called the **moment magnitude**, and it comes from the **seismic moment**. To understand the seismic moment, we need to go back to the definition of torque. A torque is a force that changes the angular momentum of a system. It is defined as the force times the distance from the center of rotation. Earthquakes are caused by internal torques, from the interactions of different blocks of the earth on opposite sides of faults. It can be shown that the moment of an earthquake is simply expressed by:

$$(\text{Moment}) = (\text{Rock Rigidity}) \times (\text{Fault Area}) \times (\text{Slip Distance})$$

Taking $M_0 = \text{Moment}$, $\mu = \text{Rock Rigidity}$, $A = \text{Fault Area}$, and $d = \text{Slip Distance}$; We can write:

$$M_0 = \mu A d$$

Both the magnitude and the seismic moment are related to the amount of energy that is radiated by an earthquake. Radiated energy is a particularly important aspect of earthquake behavior, because it causes all the damage and loss of life, and additionally, it is the greatest source of observational data. So, the seismic radiated energy is an important physical parameter to study on earthquakes. The relationships between the radiated energy, stress drop, and earthquake size provides information about the physics of the rupture process. Richter and Gutenberg, developed a relationship between magnitude and energy. Their relationship is:

$$\log_{10} [E(m)] = \frac{3}{2} m + 11.8 \quad (6)$$

It should be noted that in this relation $E(m)$ is not the total "intrinsic" energy of the earthquake. It is only the radiated energy from the earthquake and a small fraction of the total energy transferred during the earthquake process. We can write this equation in this form [3, 16],

$$\log_{10} [E(m)] = \frac{3}{2} m + \log_{10} E_0 \quad (7)$$

with $E_0 = 6.3 \times 10^4 \text{ J}$. Our aim is to determine the ratio of the total seismic energy radiated in the aftershock sequence to the seismic energy radiated in the mainshock.

This relation can be used directly to relate the radiated energy from the mainshock E_{ms} to the moment magnitude of the mainshock m_{ms} ,

$$E_{ms} = E_0 10^{3/2 m_{ms}} \quad (8)$$

We calculated the energy ratios in two ways:

The First Calculation Method To Find The Energy Ratio Among Mainshock and Aftershock Sequences:

The total radiated energy in the aftershock sequence E_{as} is obtained by integrating over the distributions of aftershocks. [3]. This can be written

$$E_{as} = \int_{-\infty}^{m_{as}^{max}} E(m) \left(-\frac{dN}{dm} \right) dm \quad (9)$$

Taking the derivative of equation (2) with respect to the aftershock magnitude m we have

$$dN = -b(\ln 10) 10^{a-bm} dm \quad (10)$$

Putting equation (10) into equation (9) gives

$$E_{as} = b(\ln 10) 10^a \int_{-\infty}^{m_{as}^{max}} E(m) 10^{-bm} dm \quad (11)$$

In addition, if we turn back to equation (8) and put it to equation (11) we get

$$E_{as} = b(\ln 10) 10^a E_0 \int_{-\infty}^{m_{as}^{max}} 10^{(3/2-b)m} dm \quad (12)$$

Then we take this integral and we find

$$E_{as} = \frac{2b}{(3-2b)} E_0 10^a 10^{(3/2-b)m_{as}^{max}} \quad (13)$$

To find the ratio of the total radiated energy in aftershocks E_{as} to the radiated energy in the mainshock E_{ms} we divide equation (13) to equation (8). Then we get the result

$$\frac{E_{as}}{E_{ms}} = \frac{2b}{(3-2b)} 10^a 10^{-bm_{as}^{max}} 10^{-3/2} (m_{ms} - m_{as}^{max}) \quad (14)$$

We know that $\Delta m = m_{ms} - m_{as}^{max}$ so equation (14) takes this form:

$$\frac{E_{as}}{E_{ms}} = \frac{2b}{(3-2b)} 10^a 10^{-bm_{as}^{max}} 10^{-3/2} \Delta m \quad (15)$$

From equation (15) the fraction of the total energy associated with aftershocks is given by

$$\frac{E_{as}}{E_{ms} + E_{as}} = \frac{1}{1 + \left(\frac{3-2b}{2b} \right) 10^{3/2} \Delta m 10^{-(a-bm_{as}^{max})}} \quad (16)$$

For the 14 earthquakes considered in the previous section we had put the b , a , Δm , and m_{as}^{max} values to equation (16) individually. Our aim is to find $\frac{E_{as}}{E_{ms} + E_{as}}$ values for 14 earthquakes considered. The obtained results are summarized in Table 3

Table 3

Summary of the Data and Results for Energy Values That Were Taken From The First Energy Calculation Method.

Earthquake	a	b	m_{as}^{max}	Δm	$\frac{E_{as}}{E_{ms} + E_{as}}$
Burdur	6.94±0.09	1.28±0.02	5.2	1.7	0.031
Plovdiv	4.11±0.17	0.68±0.03	5.6	1.4	0.013
Turkey-Iran Border	5.48±0.14	0.91±0.03	6.3	1.3	0.010
Gomati	5.27±0.13	0.85±0.02	5.9	1.2	0.036
Canakkale-Yenice	4.79±0.12	0.83±0.02	5.4	1.8	0.005
Bolu-Abant	3.83±0.05	0.61±0.01	5.9	1.2	0.018
Mus-Varto	5.18±0.25	0.93±0.05	5.3	1.6	0.011
Adapazarı-Mudurnu	6.56±0.19	1.20±0.04	5.4	1.8	0.010
Thessaloniki	4.38±0.14	0.81±0.05	4.7	1.4	0.034
Racha	5.12±0.16	0.95±0.03	5.0	1.2	0.060
Cyprus	5.99±0.07	1.11±0.01	5.3	1.5	0.020
Adana-Ceyhan	3.52±0.13	0.67±0.03	5.1	1.2	0.016
Kocaeli-Golcuk	4.94±0.15	0.90±0.03	5.8	1.6	0.003
Duzce	4.98±0.09	0.83±0.02	5.4	1.8	0.008

For the earthquakes that are on NAFZ, we find the mean energy $\frac{E_{as}}{E_{ms} + E_{as}} = 0.009$

with a standard deviation $\sigma_{\bar{E}} = 0.005$. Consequently, we find that for these earthquakes on average about 99.1 per cent of the available elastic energy is released during the mainshock and about 0.9 per cent of energy is released during the aftershocks.

For the earthquakes that are on Aegean Graben System, we find the mean energy $\frac{E_{as}}{E_{ms} + E_{as}} = 0.029$ with a standard deviation $\sigma_{\bar{E}} = 0.011$. Consequently, we find that for these earthquakes on average about 97.1 per cent of the available elastic energy is released during the mainshock and about 2.9 per cent of energy is released during the aftershocks.

For the earthquakes that are on Cyprus Arc Zone, we find the mean energy

$\frac{E_{as}}{E_{ms} + E_{as}} = 0.018$ with a standard deviation $\sigma_{\bar{E}} = 0.003$. Consequently, we find that

for these earthquakes on average about 98.2 per cent of the available elastic energy is released during the mainshock and about 1.8 per cent of energy is released during the aftershocks.

The Second Calculation Method To Find The Energy Ratio Among Mainshock and Aftershock Sequences:

Additionally, from the study of Turcotte and Shcherbakov in 2004 [3,4], we derive the same relationship in terms of b and Δm^* values.

The total radiated energy in the aftershock sequence E_{as} is obtained by integrating over the distributions of aftershocks [3,4]. This can be written

$$E_{as} = \int_{-\infty}^{m^*} E(m) \left(-\frac{dN}{dm} \right) dm \quad (9)$$

Taking the derivative of equation (5) with respect to the aftershock magnitude m we have

$$dN = -b(\ln 10) 10^{b(m_{ms} - \Delta m^* - m)} dm \quad (17)$$

Putting equation (17) into equation (9) gives

$$E_{as} = b(\ln 10) 10^{b(m_{ms} - \Delta m^*)} \int_{-\infty}^{m^*} E(m) 10^{-bm} dm \quad (18)$$

In addition, if we turn back to equation (8) and put it to equation (18) we get

$$E_{as} = b(\ln 10) 10^{b(m_{ms} - \Delta m^*)} E_0 \int_{-\infty}^{m^*} 10^{(3/2-b)m} dm \quad (19)$$

Then we take this integral and we find

$$E_{as} = \frac{2b}{(3-2b)} E_0 10^{(3/2-b)m^*} 10^{b(m_{ms} - \Delta m^*)} \quad (20)$$

Using equation (4) we find

$$E_{as} = \frac{2b}{(3-2b)} E_0 10^{3/2(m_{ms} - \Delta m^*)} \quad (21)$$

To find the ratio of the total radiated energy in aftershocks E_{as} to the radiated energy in the mainshock E_{ms} we divide equation (21) to equation (8). Then we get the result

$$\frac{E_{as}}{E_{ms}} = \frac{2b}{(3-2b)} 10^{-3/2 \Delta m^*} \quad (22)$$

If we further assume that all earthquakes have the same seismic efficiency (ratio of radiated energy to the total drop in stored elastic energy), then this ratio is also the ratio of

the drop in stored elastic energy due to the aftershocks to the drop in stored elastic energy due to the mainshock. From equation (22) the fraction of the total energy associated with aftershocks is given by

$$\frac{E_{as}}{E_{ms} + E_{as}} = \frac{1}{1 + \frac{3-2b}{2b} 10^{3/2} \Delta m^*} \quad (23)$$

For the 14 earthquakes considered in the previous section we had put the b and Δm^* values to equation (23) individually. Our aim is to find $\frac{E_{as}}{E_{ms} + E_{as}}$ values for 14 earthquakes considered. The obtained results are summarized in Table 4.

Table 4
Summary of the Data and Results for Energy Values That Were Taken From The Second Energy Calculation Method.

Earthquake	b	Δm^*	$\frac{E_{as}}{E_{ms} + E_{as}}$
Burdur	1.28±0.02	1.46±0.11	0.036
Plovdiv	0.68±0.03	0.97±0.38	0.028
Turkey-Iran Border	0.91±0.03	1.57±0.24	0.007
Gomati	0.85±0.02	0.92±0.19	0.052
Canakkale-Yenice	0.83±0.02	1.41±0.22	0.009
Bolu-Abant	0.61±0.01	0.85±0.12	0.035
Mus-Varto	0.93±0.05	1.32±0.39	0.016
Adapazarı-Mudurnu	1.20±0.04	1.75±0.23	0.009
Thessaloniki	0.81±0.05	0.70±0.35	0.095
Racha	0.95±0.03	0.80±0.23	0.098
Cyprus	1.11±0.01	1.42±0.09	0.021
Adana-Ceyhan	0.67±0.03	1.05±0.28	0.021
Kocaeli-Golcuk	0.81±0.04	1.49±0.34	0.007
Duzce	0.83±0.02	1.17±0.18	0.021

For the earthquakes that are on NAFZ, we find the mean energy $\frac{E_{as}}{E_{ms} + E_{as}} = 0.015$ with a standard deviation $\sigma_{\bar{E}} = 0.012$. Consequently, we find that for these earthquakes on average about 98.5 per cent of the available elastic energy is released during the mainshock and about 1.5 per cent of energy is released during the aftershocks.

For the earthquakes that are on Aegean Graben System, we find the mean energy

$\frac{E_{as}}{E_{ms} + E_{as}} = 0.053$ with a standard deviation $\sigma_{\bar{E}} = 0.030$. Consequently, we find that

for these earthquakes on average about 94.7 per cent of the available elastic energy is released during the mainshock and about 5.3 per cent of energy is released during the aftershocks.

For the earthquakes that are on Cyprus Arc Zone, we find the mean energy

$\frac{E_{as}}{E_{ms} + E_{as}} = 0.021$ with no standard deviation. Consequently, we find that for these

earthquakes on average about 97.9 per cent of the available elastic energy is released during the mainshock and about 2.1 per cent of energy is released during the aftershocks.

Conclusions

Earthquakes occur in clusters. After one earthquake happens, we usually see others at nearby or identical location. Clustering of earthquakes usually occurs near the location of the mainshock. The stress on the mainshock's fault changes drastically during the mainshock and that fault produces most of the aftershocks. This causes a change in the regional stress, the size of which decreases rapidly with distance from the mainshock. Sometimes the change in stress caused by the mainshock is great enough to trigger aftershocks on other, nearby faults. It is accepted that aftershocks are caused by stress transfer during an earthquake. When an earthquake occurs there are adjacent regions where the stress is increased. The relaxation of these stresses causes aftershocks [3, 17, 18, 19, 20, 21, 22].

Several scaling laws are also found to be universally valid for aftershocks [2, 3, 4]. These are:

- (1) Gutenberg-Richter frequency-magnitude scaling
- (2) Båth's law for the magnitude of the largest aftershock
- (3) The modified Omori's law for the temporal decay of aftershocks

In this article we are using both Båth's law and G-R scaling. Our aim is to find an upper cutoff magnitude m^* for a given aftershock sequence. Using relation (3), we get related a and b values in the G-R scaling. Båth's law states that, to a good approximation, the difference in magnitude between mainshock and its largest aftershock is a constant independent of the mainshock magnitude. We obtain values for the difference between the mainshock magnitude m_{ms} and the largest detected aftershock magnitude m_{as}^{max} for the 14 large earthquakes. This difference is known as Δm and we also obtain values for the difference between the mainshock magnitude m_{ms} and the "largest" inferred aftershock m^* . This difference is known as Δm^* .

A modified form of Båth's law was proposed by Turcotte and Shcherbakov in 2004. They considered 10 large earthquakes that occurred in California between 1987 and 2003 with magnitudes equal to or greater than $m_{ms} \geq 5.5$. According to their theory the mean difference in magnitudes between these mainshocks and their largest detected aftershocks is 1.16 ± 0.46 . This result is consistent with Båth's Law. They found the mean difference in magnitudes between the mainshocks and their largest inferred aftershocks is 1.11 ± 0.29 . They also calculated the partitioning of energy during a mainshock-aftershock sequence and

found that about 96 per cent of the energy dissipated in a sequence is associated with the mainshock and the rest (4 per cent) is due to aftershocks. Their results are given in Table 5. During their calculation process they did not make any classification among these ten large earthquakes that occurred in California. We applied the Modified Form of Båth's Law to our 14 large earthquakes that occurred in and near boundary neighbors of Turkey. We followed the same calculation process. But we also made additional analysis on these earthquakes. Because Turkey has different fault zones, we needed to make a classification among all 14 earthquakes. According to our classification, six earthquakes take place on the North Anatolian Fault Zone (NAFZ). Four earthquakes are on Aegean Graben System. Two earthquakes take place on Cyprus Arc Zone. One earthquake is on the East Anatolian Fault Zone (EAFZ), and one earthquake is in Georgia.

Table 5
Summary of the Results of Turcotte and Shcherbakov

Parameters	Turcotte and Shcherbakov
$\overline{\Delta m}$	1.16 ± 0.46
Δm^*	1.11 ± 0.29
$\frac{E_{as}}{E_{ms} + E_{as}}$	0.038

Table 6
Summary of Our Results

Parameters	NAFZ	Aegean Graben System	Cyprus Arc Zone
$\overline{\Delta m}$	1.63 ± 0.23	1.43 ± 0.21	1.35 ± 0.21
Δm^*	1.20 ± 0.08	1.30 ± 0.09	1.39 ± 0.09
$\frac{E_{as}}{E_{ms} + E_{as}}$	0.015	0.030	0.021

Table 6 shows all results that we got from this study. According to Table 6, for the North Anatolian Fault Zone (NAFZ), a large fraction of the accumulated energy is released in the mainshock and only a relatively small fraction of the accumulated energy is released in the aftershock sequence. The results of Turcotte and Shcherbakov are for the ten earthquakes in California on the San Andreas Fault Zone. Although SAFZ (in California) and NAFZ (in Turkey) have the same seismic properties, the released energy during the mainshocks in the NAFZ is much greater than the released energy during the mainshocks in the SAFZ.

Additionally, Figure 4 gives us the relation between Δm and Δm^* . In this figure, line 1 shows the harmony of our data with the Båth's Law. According to Figure 4, our data do not show harmony with the Båth's Law. Båth's Law states that the difference in magnitude between a mainshock and its largest detected aftershock is constant, regardless of the mainshock magnitude and it is about 1:2 [3, 4, 7, 8]. But in Figure 4, only four earthquakes

have Δm values equal to 1:2. The other ten earthquakes have Δm values greater than 1:2. Consequently, only 29 per cent of our data show harmony with the Båth's Law. The rest part (71 per cent) of our data do not show harmony with the Båth's Law.

The constancy of the differences in magnitudes between mainshocks and their largest aftershocks is an indication of scale-invariant behavior of aftershock sequences. In Figure 4, line 2 shows the harmony of our data with the Modified Form of Båth's Law. This line corresponds to $y = x$ line. If the Modified Form of Båth's Law gave us perfect results, Δm and Δm^* values would be close to each other along this line. Hence, they would be the near of line 2. But in Figure 4, only two earthquakes take place on the upper side of this line. The remaining 12 earthquakes take place on the lower side of this line. Consequently, our data do not show harmony with the Modified Form of Båth's Law.

The other important conclusion is that we know most of the energy is released during the mainshock. Therefore, after the mainshock the community and government may begin their work to rescue people from the debris without wasting any time.

References

- [1] Kanamori, H. and Emily E. Brodsky, "The physics of earthquakes", *Reports on Progress in Physics* Vol. 67, pp. 1429-1496, 2004.
- [2] Kisslinger, C., "Aftershocks and fault-zone properties", *Advances in Geophysics* Vol. 38, pp. 1-36, 1996.
- [3] Shcherbakov, R. and Donald L. Turcotte, "A Modified Form Of Båth's Law", *Bulletin of the Seismological Society of America*, Vol. 94, No. 5, pp. 1968-1975, 2004.
- [4] Shcherbakov, R., Donald L. Turcotte, and John B. Rundle, "Aftershock Statistics", *Pure and Applied Geophysics*, Vol. 162, pp. 1051-1076, 2005.
- [5] Gutenberg, B. and C. F. Richter, "Seismicity of the Earth and Associated Phenomena", Princeton Univ. Press, Princeton, New Jersey, 1954.
- [6] Omori, F., "On the aftershocks of earthquakes", *Journal of College of Science of the Imperial University of Tokyo*, Vol. 7, pp. 111-200, 1894.
- [7] Helmstetter, A. and D. Sornette, "Båth's law Derived from the Gutenberg- Richter law and from Aftershock Properties", *Geophysical Research Letters*, Vol. 30, doi:10.1029/2003GL018186, 2003.
- [8] Båth, M., "Lateral inhomogeneities of the upper mantle", *Tectonophysics*, Vol. 2, pp. 483-514, 1965.
- [9] Kagan, Y. Y. and L. Knopoff, "Stochastic synthesis of earthquake catalogs", *Journal of Geophysical Research*, Vol. 86, pp. 2853-2862, 1981.
- [10] Ogata, Y., "Statistical models for earthquake occurrence and residual analysis for point processes", *Journal of the American Statistical Association*, Vol 83, pp. 9-27, 1988.
- [11] Frolich, C., and S. D. Davis, "Teleseismic b values; or much ado about 1.0", *Journal of Geophysical Research*, Vol. 98, pp. 631-644, 1993.
- [12] Bogazici University Kandilli Observatory and Earthquake Research Institute, <http://www.koeri.boun.edu.tr>, 2006.
- [13] Molchan, G. M. and O. E. Dmitrieva, "Aftershock identification: methods and ne approaches", *Geophysical Journal International* Vol. 109, pp. 501-516, 1992.
- [14] Kagan, Y. Y., "Aftershock zone scaling", *Bulletin of Seismological Society of America* Vol. 92, pp. 641-655, 2002.
- [15] Taymaz, T., O. Tan and S. Yolsal, "Active Tectonics of Turkey and Surroundings and Seismic Risk in the Marmara Sea Region", _Istanbul Technical University, Faculty of Mines, Department of Geophysics, Seismology Section.

- [16] Utsu, T., "Relationship between magnitude scales", in International Handbook of Earthquake and Engineering Seismology, W. H. K., 2002.
- [17] Rybicki, K., "Analysis of aftershocks on the basis of dislocation theory", *Physics of the Earth and Planetary Interiors*, Vol. 7, pp. 409-422, 1973.
- [18] Das S. and C. H. Scholz, "Off-fault aftershock clusters caused by shear stress increase?", *Bulletin of Seismological Society of America*, Vol. 71, pp. 1669-1675, 1981.
- [19] Mendoza, C., and S. H. Hartzell, "Aftershock patterns and main shock faulting", *Bulletin of Seismological Society of America*, Vol. 78, 1438-1449, 1988.
- [20] King, G. C. P., R. S. Stein and J. Lin, "Static stress changes and the triggering of earthquakes", *Bulletin of Seismological Society of America*, Vol. 84, pp. 935-953, 1994.
- [21] Marcellini, A., "Arrhenius behavior of aftershock sequences", *Journal of Geophysical Research* Vol. 100, pp. 6463-6468, 1995.
- [22] Hardebeck, J. L., J. J. Nazareth and E. Hauksson, "The static stress change triggering model: constraints from two southern California aftershock sequences", *Journal of Geophysical Research*, Vol. 103, pp. 24,427-24,437, 1998.